Exchange Control of Nuclear Spin Diffusion in a Double Quantum Dot

Exchange Control of Nuclear Spin Diffusion in a Double Quantum Dot

D. J. Reilly,[1,5] J. M. Taylor,[2] J. R. Petta,[3] C. M. Marcus,[1] M. P. Hanson,[4] and A. C. Gossard[4]

[1]*Department of Physics, Harvard University, Cambridge, Massachusetts 02138, USA*
[2]*Department of Physics, Massachusetts Institute of Technology, Cambridge, Massachusetts 02139, USA*
[3]*Department of Physics, Princeton University, Princeton, New Jersey 08544, USA*
[4]*Department of Materials, University of California, Santa Barbara, California 93106, USA*
[5]*School of Physics, The University of Sydney, Sydney, NSW 2006, Australia*

(Received 20 January 2009; published 8 June 2010)

The influence of gate-controlled two-electron exchange on the relaxation of nuclear polarization in small ensembles ($N \sim 10^6$) of nuclear spins is examined in a GaAs double quantum dot system. Waiting in the (2,0) charge configuration, which has large exchange splitting, reduces the nuclear diffusion rate compared to that of the (1,1) configuration. Matching exchange to Zeeman splitting significantly increases the nuclear diffusion rate.

DOI: 10.1103/PhysRevLett.104.236802 PACS numbers: 73.21.La, 71.70.Jp

Precise control of single electron spins in quantum dots [1] can be used to provide a comparable degree of control of the polarization of small ensembles of nuclei, which couple to single confined electrons via the hyperfine interaction [2–5]. Ultimately, this control may provide a means of storing spin-based quantum information in nuclear ensembles [6,7]. The simplest such process is the induction of an out-of-equilibrium average polarization of the nuclear ensemble by dynamic nuclear polarization (DNP), where the ''flip'' of a polarized electron spin is accompanied by the ''flop'' of a nuclear spin [8]. In recent years, experimental studies of DNP have been extended from bulk systems [9,10] to the nanoscale [11–13], including quantum dots containing a small number of electrons [2–4,14–17]. DNP driven by spin-blocked transport can create feedback that leads to hysteretic and complex time-dependent currents [18–23], while gate-driven DNP leads to a simpler buildup of nuclear polarization, often saturating at surprisingly small levels [3,4].

This Letter reports time-dependent measurements of the induction and relaxation of DNP in a few-electron double quantum dot as a function of magnetic field and electron arrangement in the double dot. Cyclic evolution of the two-electron spin state, driven by gate pulses [3], repeatedly flops nuclear spins to create a small local DNP of order 1%. Relaxation is monitored by detecting the Overhauser field using high-bandwidth charge sensing [24]. In this work, it is shown that nuclear diffusion is sensitive to the exchange coupling of confined electrons, controlled experimentally through the spatial charge arrangement with fixed total charge. We find that electron-mediated coupling of nuclear spins [8,25] dominates nuclear diffusion.

The double dot is formed by Ti/Au gates patterned with electron beam lithography on the surface of a $GaAs/Al_{0.3}Ga_{0.7}As$ heterostructure with two-dimensional electron gas with density 2×10^{15} m^{-2} and mobility 20 m^2/V s, as shown in Fig. 1(a). Measurements were made in a dilution refrigerator at the base electron temperature of $\sim$120 mK. A schematic energy-level diagram of the two-electron system is shown in Fig. 1(b), with the labels (n, m) giving the number of electrons in the left and right dots. Quasistatic gate voltages control interdot tunnel coupling t_c, while the detuning ϵ from the (2,0)-(1,1) charge degeneracy is controlled by fast (nanosecond scale) voltage pulses [Fig. 1(a)]. The charge configuration of the double dot is detected by monitoring the conductance G_{QPC} of an rf quantum point contact (rf QPC). G_{QPC} controls the reflected power Γ_{rf} of a 220 MHz rf carrier; following demodulation, this yields a voltage V_{rf} that constitutes the charge sensing signal [24].

The mean total effective field experienced by electrons in (1,1) is $\mathbf{B}_{\mathrm{tot}} = \mathbf{B}_0 + \mathbf{B}_{\mathrm{nuc}}$, where $\mathbf{B}_0$ is the external field applied perpendicular to the two-dimensional electron gas plane and $\mathbf{B}_{\mathrm{nuc}} = (\mathbf{B}^{\mathrm{L}}_{\mathrm{nuc}} + \mathbf{B}^{\mathrm{R}}_{\mathrm{nuc}})/2$ is the Overhauser field averaged over left and right dots, due to $N \sim 10^6$ nuclear spins. The avoided crossing between the singlet (S) and the (1,1) $m_s = 1$ triplet (T_+) occurs at a value of ϵ [thick, green arrow in Fig. 1(b)] set by the total Zeeman energy, $E_{\mathrm{tot}} = g\mu_B B_{\mathrm{tot}}$, where $g \simeq -0.4$ is the electron g factor in GaAs, μ_B is the Bohr magneton, and B_{tot} is the magnitude of $\mathbf{B}_{\mathrm{tot}}$. The gap and width of the avoided crossing are set by $E^{\perp}_{\mathrm{nuc}} = g\mu_B \Delta B^{\perp}_{\mathrm{nuc}}$, where $\Delta B^{\perp}_{\mathrm{nuc}}$ is the magnitude of the component of $\Delta\mathbf{B}_{\mathrm{nuc}} = (\mathbf{B}^{\mathrm{L}}_{\mathrm{nuc}} - \mathbf{B}^{\mathrm{R}}_{\mathrm{nuc}})/2$ transverse to B_{tot}.

We probe the S-T_+ resonance using the pulse sequence shown in Fig. 2(b), which first prepares $(2, 0)S$ at (P) then separates the electrons (S) for a time τ_{S} before returning to (2,0) for measurement (M) for time $\tau_{\mathrm{M}} \sim 5$ μs. The Pauli spin blockade ensures that only the (1,1) singlet returns to (2,0), with triplets blocked for a time T_1. In this way, the two-electron spin state is mapped to a charge configuration that is detected with the rf QPC. Cycling this sequence yields a feature at (M) in the (2,0) region, indicated by white lines in Fig. 1(c). Once calibrated, V_{rf} gives the probability $1\text{-}P_S$ that an initial singlet evolved into T_+ during the separation interval τ_{S}. Fitting the time-averaged function $P_S(\tau_{\mathrm{S}})$ gives an inhomogeneous dephasing time,

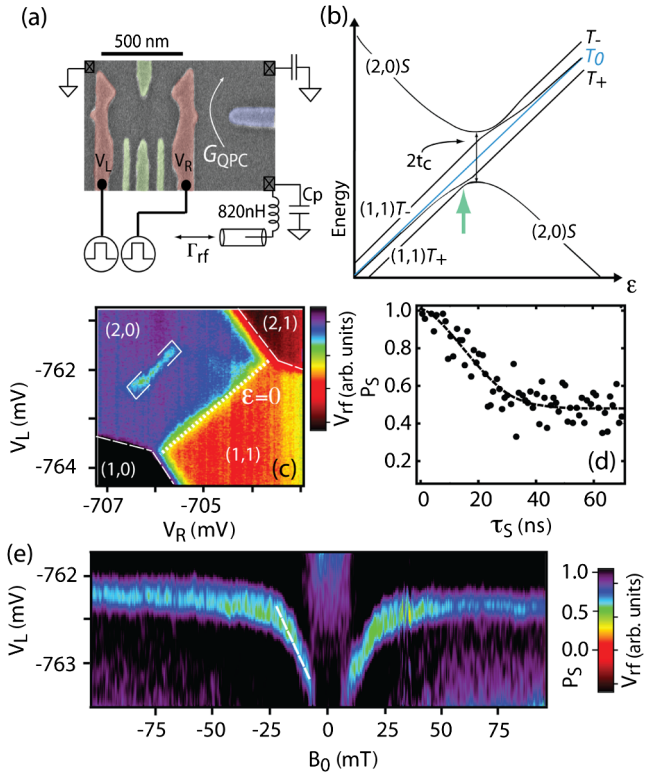

FIG. 1 (color online). (a) False-color SEM image of a representative double dot with an integrated rf-QPC charge sensor. (b) Energy-level diagram of the two-electron system. The green arrow points to the S-T_+ avoided crossing. (c) V_{rf} around the (2,0)-(1,1) charge transition during cycling of the probe sequence. A plane has been subtracted. The region indicated with white lines corresponds to the S-T_+ resonance. $B_0 = 8$ mT. (d) Singlet return probability P_S as a function of separation time τ_S, yielding a $T_2^* \sim 15$ ns. $B_0 = 8$ mT, $\tau_M = 1.6$ μs. The black dashed line is a fit to the theoretical Gaussian form [35]. (e) P_S as a function of the left gate bias V_L and magnetic field B_0. The dashed line converts the position of the resonance in V_L to B_{tot}.

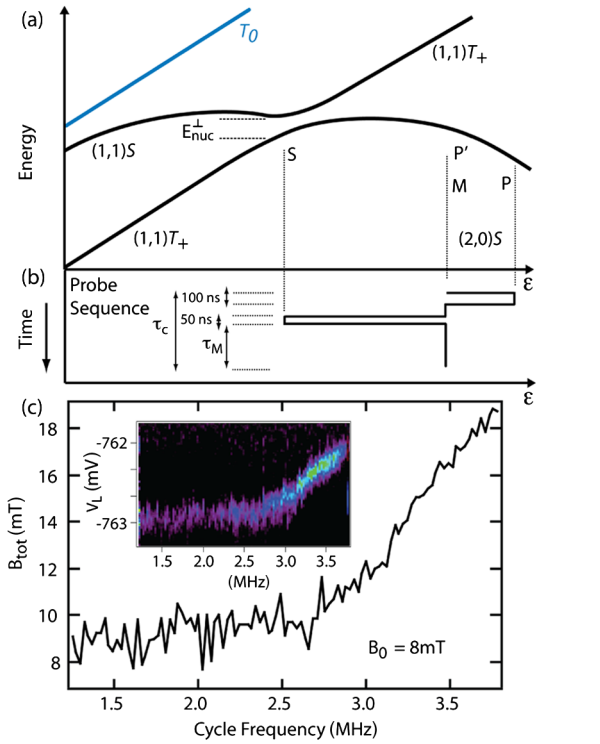

FIG. 2 (color online). (a) Energy-level diagram near the S-T_+ resonance. (b) Pulse cycle used to measure the position of the resonance during the probe sequence. (c) Inset: Position of the S-T_+ resonance with respect to the gate bias, V_L. The color scale is the same as Fig. 1(e). For cycle rates below 1 MHz, the position of the resonance indicates $B_{tot} \sim B_0$; i.e., no appreciable polarization is established by the process of measuring the position of the S-T_+ resonance. The main panel shows the position of the resonance converted to units of B_0 via the calibration in Fig. 1(e).

$T_2^* \sim 15$ ns. The dependence of the S-T_+ resonance position (in V_L, with V_R fixed) on B_0 in the range $B_0 =$ 5–18 mT, in the absence of a polarization, serves as a calibration to determine B_{tot} when nuclear polarization is present [26].

DNP is investigated using a three-step "pump-pause-probe" sequence: The pump sequence starts from a singlet in (2,0) then moves adiabatically through the S-T_+ resonance, flipping an electron and flopping a nuclear spin—in principle, once per cycle at a rate of 4 MHz [3]. The "probe" sequence [Figs. 2(a) and 2(b)] also starts with a singlet in (2,0) but moves to the S-T_+ resonance, providing a measure of B_{tot}. A cycle rate of 200 kHz is used for the probe sequence and does not induce DNP, as seen in Fig. 2(c). Pump and probe cycles are separated by a static "pause" of duration Δt.

The pump sequence creates a steady-state DNP of order ~10 mT, which, in the absence of a pause, relaxes during the probing cycle on a time scale $\tau_R = 8$ s, found by fitting an exponential to $B_{tot}(t)$ [Fig. 3(c)]. Increasing B_0 from 8 mT to 10 mT doubles the time taken for B_{tot} to return to B_0. This increase in τ_R with B_0 saturates above $B_0 \sim$ 10 mT, so that there is little change in relaxation time at $B_0 = 15$ mT compared to the $B_0 = 10$ mT data, consistent with the measured field dependence of nuclear fluctuations [27]. We also note that at $t = 0$, B_{tot} appears nearly independent of B_0. This suggests that the pump sequence ceases to produce polarization above a certain value of B_{tot}, qualitatively consistent with previous measurements [3]. The measured relaxation rate cannot account for the small steady-state polarization (~10 mT), and we are led to conclude that there must be a significant decrease in the efficiency of the polarization cycle with increasing B_{nuc}.

The effect of pausing in (2,0) between the pump and probe sequences can be seen in Fig. 4(b), which shows that more than half the polarization remains after pausing for 30 s in $(2,0)S$ [Fig. 4(c)]. Once the probe sequence is initiated after the pause, B_{tot} once again decays with $\tau_R \sim 8$ s. The influence of the probe sequence is examined further by introducing multiple pause intervals in (2,0), interleaved with probe cycles [Fig. 4(d)].

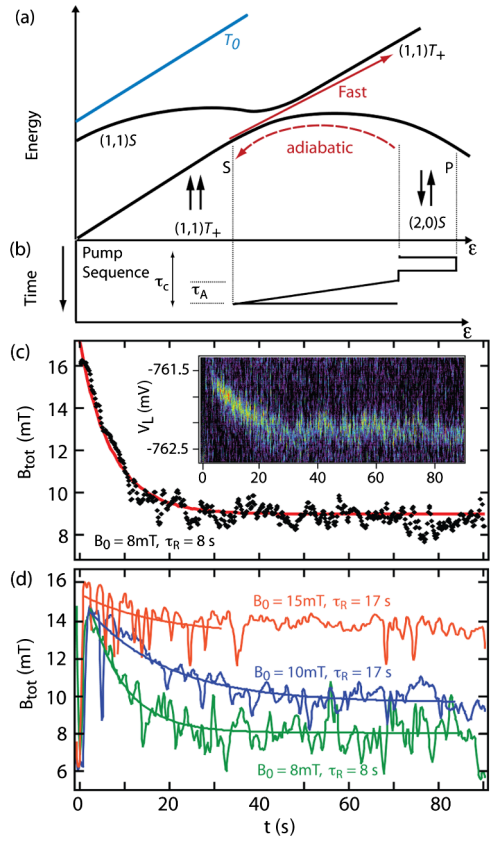

FIG. 3 (color online). (a) Energy-level diagram near the S-T_+ avoided crossing with a pump sequence used to create the DNP shown in (b), $\tau_A = 50$ ns, $\tau_c = 250$ ns. The pump cycle rate is 4 MHz. (c) Inset: Decay in the position of the resonance with respect to V_L following pumping. The main panel shows the average of five pump-probe sequences, with B_{tot} calibrated using Fig. 1(e). The red solid curve is an exponential fit. (d) Relaxation of DNP at $B_0 = 8$ mT (lower green curve) $\tau_R = 8 \pm 2$ s, $B_0 = 10$ mT (middle blue curve) $\tau_R = 17 \pm 3$ s, and $B_0 = 15$ mT (upper red curve) $\tau_R = 17 \pm 5$ s.

The dependence of the nuclear relaxation time τ_R on the two-electron spin state during the pause duration is shown in Fig. 4(f). Pausing for the duration of Δt in the (2,0) state yields $\tau_R = 56$ s [red data in Fig. 4(f)], while pausing in (1,1) yields $\tau_R = 26$ s [green data in Fig. 4(f)]. We ascribe these different relaxation times to a nuclear spin diffusion constant that depends on the two-electron spin state. With diffusion dominated by the shortest dimension of the dot, perpendicular to the electron gas, we approximate the diffusion constant $D = \sigma_z^2/\tau_R$ based on an estimate of the width of the wave function, $\sigma_z \sim 7$ nm. This gives $D \sim 1 \times 10^{-14}$ cm^2 s^{-1} for the case of pausing in (2,0), consistent with earlier optical measurements of nuclear diffusion in GaAs [10]. Activation of the probe sequence increases diffusion to $D \sim 7 \times 10^{-14}$ cm^2 s^{-1}.

The presence of strongly confined electrons is expected to affect nuclear spin diffusion in two opposing ways. Suppressing diffusion, electrons couple nonuniformly with the nuclei and create an inhomogeneous Knight shift [28], lifting the degeneracy between nuclear dipoles and preventing them from flip-flopping with each other. The Knight shift gives rise to a frequency shift of order $\lambda_i = A v_0/h|\psi(\mathbf{r_i})|^2$ for nuclear spin at position $\mathbf{r_i}$, electron wave function ψ, and hyperfine constant A, (v_0 is the unit cell volume for GaAs and h is Planck's constant). The change of this shift from site to site in the lattice is given by $[|\psi(r_i + a)|^2 - |\psi(r_i)|^2] \sim \vec{a}\,\vec{\nabla}\,|\psi(r)|^2|_{r=r_i}$, where a is the lattice constant. A wave function $\psi(x, y, z) = \phi(x, y)(2\sigma_z^{-3/2} e^{-z/\sigma_z})$ gives a maximum gradient of the Knight shift of $\frac{A v_0}{h}|\phi(x, y)|^2 0.92\sigma_z^{-2}$. For a nearest-neighbor distance of like species of 0.565 nm$/\sqrt{2}$ (like species are in a fcc lattice, $a = 0.565$ nm), we find a Knight shift gradient of 15% of the maximum Knight shift, i.e., $0.15A/N \approx 2$ kHz. This Knight shift is comparable to the random gradient associated with the nuclear dipole-dipole field.

Alternatively, electrons can enhance diffusion via the virtual process of electron-mediated nuclear spin exchange which couples distant nuclear spins [8,25]. To estimate the strength of this process we consider the nuclear field (with rms strength B_{nuc}) due to the transverse components of the nuclear spins $B_{\mathrm{nuc}} \propto \sum_j \lambda_j I_+^j$. This fluctuating field virtually flips the electron spin with a coupling $\sim \lambda\sqrt{N} = g\mu_B B_{\mathrm{nuc}}$, which flops back while flipping nuclear spin i with a coupling λ_i. The process is suppressed by the electron Zeeman energy, $g\mu_B B_{\mathrm{tot}}$, giving an effective transverse magnetic field felt by nuclear spin $i \sim (\hbar\gamma_i)^{-1}\lambda_i \frac{B_{\mathrm{nuc}}}{B_{\mathrm{tot}}}$, where γ_i is the gyromagnetic ratio of spin i. Using the specific values for our device, with $N \simeq 6 \times 10^6$ nuclear spins, we find that an enhancement over the intrinsic dipolar field occurs for $B_{\mathrm{tot}} \lesssim 10 B_{\mathrm{nuc}} \sim 20$ mT.

Thus, the enhancement of diffusion via electron-mediated spin flips in the (1,1) state dominates the suppression due to the Knight shift, leading to an overall increase in nuclear spin diffusion. However, with electrons in $(2, 0)S$, both hyperfine mechanisms are suppressed by the electron exchange energy J, which is 10^4 times larger than $g\mu_B B_{\mathrm{tot}}$ for the fields used. In $(2, 0)S$ the right dot is unoccupied, and in the case of the left dot, the large J ensures that electron-mediated (enhanced) diffusion is a negligible contribution. The result is that for $(2, 0)S$, the dynamics of B_{tot} is dominated by the bare nuclear dipole-dipole diffusion of polarization from both dots [29]. Consistent with this mechanism, limited data taken during pausing in the (1,0) configuration yielded a similar relaxation time to pausing in (1,1).

Electron-mediated flipping leads to an increase in diffusion with decreasing B_{tot}, in keeping with the B_0 dependence of the data shown in Fig. 3(d). Nonsecular corrections to the nuclear dipole-dipole interaction will also enhance diffusion for $B_{\mathrm{tot}} \lesssim 1$ mT [2,8]. Flipping of nuclear spins via electron cotunneling processes is an additional mechanism that can lead to decay of the polarization; however, for the gate biases used in this experiment,

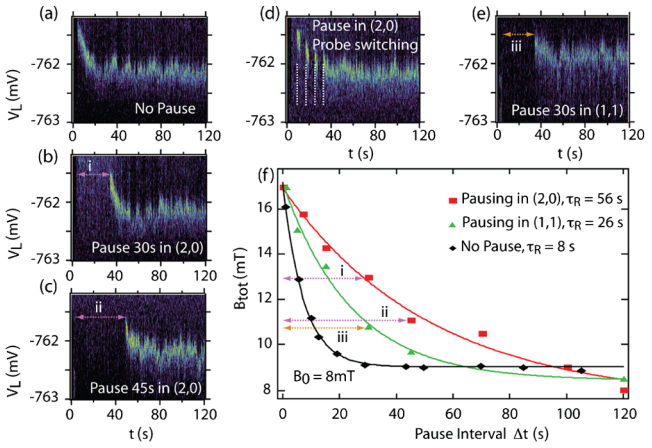

FIG. 4 (color online). (a) Immediate decay in the position of the resonance during the probe sequence. (b) Decay in the position of the resonance following a pause interval of 30 s in (2,0) between the pump and probe sequences. Pausing in (2,0) suppresses hyperfine coupling. (c) Same as (b), but with the pause interval set to 45 s. (d) Decay of the resonance during probing, interleaved with multiple pause intervals. (e) Decay in the position of the resonance following a pause of 30 s in (1,1). (f) Decay of B_{tot} as a function of the pause interval Δt and for different configurations of a two-electron spin state.

this contribution is expected to be negligible. Varying the tunnel barriers to the leads while keeping the number of electrons on each dot fixed in (2,0) or (1,1) produced little variation in decay time of the polarization. At the S-T_+ resonance, the exchange energy is effectively ''canceled'' by the Zeeman energy, allowing rapid flipping of electrons that readily mediate rapid exchange of nuclear spins. This is the likely explanation for the enhanced diffusion observed during the probe sequence.

For our double-dot system, the largest nuclear polarization achievable using a gate pump sequence was shown to be $\sim$1% [3]. Based on our measurement of τ_R, we emphasize that this maximum steady-state DNP cannot be limited by rapid diffusion of polarization out of the dots. Rather, these results indicate that the pump sequence strongly decreases in efficiency with increasing polarization. Such a scenario is consistent with the idea of dark state formation [30], in which the nuclear system is driven to a configuration where it does not interact with the electron spins used in the pump sequence. Hyperfine-mediated nuclear dynamics in quantum dots have been considered theoretically in the context of spin-preserving processes [25,31–34], but measurements of the nuclear relaxation in systems that allow for the removal of a single electron have only recently been reported [2]. For two-electron systems, the measurements presented here bring to light the role of electron exchange, which, as we have shown, can lead to a suppression of hyperfine-mediated nuclear spin diffusion.

We thank L. DiCarlo, A. Johnson, and E. Laird for technical contributions. We thank W. Coish, F. Koppens, D. Loss, and A. Yacoby for useful discussions. This work was supported by ARO/IARPA, DARPA, NSF-NIRT (EIA-0210736), the Harvard CNS, and the Pappalardo grant program (J. M. T.). Research at UCSB was supported in part by QuEST, an NSF Center.

[1] R. Hanson, L. P. Kouwenhoven, J. R. Petta, S. Tarucha, and L. M. K. Vandersypen, Rev. Mod. Phys. **79**, 1217 (2007).
[2] P. Maletinsky, A. Badolato, and A. Imamoglu, Phys. Rev. Lett. **99**, 056804 (2007).
[3] J. R. Petta *et al.*, Phys. Rev. Lett. **100**, 067601 (2008).
[4] S. Foletti, J. Martin, M. Dolev, D. Mahalu, V. Umansky, and A. Yacoby, arXiv:0801.3613.
[5] D. J. Reilly *et al.*, Science **321**, 817 (2008).
[6] J. M. Taylor, C. M. Marcus, and M. D. Lukin, Phys. Rev. Lett. **90**, 206803 (2003).
[7] W. M. Witzel and S. Das Sarma, Phys. Rev. B **76**, 045218 (2007).
[8] A. Abragam, *Principles of Nuclear Magnetism*, International Series of Monographs on Physics, Vol. 32 (Oxford University Press, New York, 1983).
[9] G. Lampel, Phys. Rev. Lett. **20**, 491 (1968).
[10] D. Paget, Phys. Rev. B **25**, 4444 (1982).
[11] G. Salis *et al.*, Phys. Rev. Lett. **86**, 2677 (2001).
[12] K. Wald *et al.*, Phys. Rev. Lett. **73**, 1011 (1994).
[13] M. Dobers *et al.*, Phys. Rev. Lett. **61**, 1650 (1988).
[14] D. Gammon *et al.*, Phys. Rev. Lett. **86**, 5176 (2001).
[15] C. W. Lai *et al.*, Phys. Rev. Lett. **96**, 167403 (2006).
[16] A. I. Tartakovskii *et al.*, Phys. Rev. Lett. **98**, 026806 (2007).
[17] E. A. Laird *et al.*, Phys. Rev. Lett. **99**, 246601 (2007).
[18] K. Ono and S. Tarucha, Phys. Rev. Lett. **92**, 256803 (2004).
[19] F. H. L. Koppens *et al.*, Science **309**, 1346 (2005).
[20] J. Baugh *et al.*, Phys. Rev. Lett. **99**, 096804 (2007).
[21] O. N. Jouravlev and Y. V. Nazarov, Phys. Rev. Lett. **96**, 176804 (2006).
[22] M. S. Rudner and L. S. Levitov, Phys. Rev. Lett. **99**, 246602 (2007).
[23] H. O. H. Churchill *et al.*, Nature Phys. **5**, 321 (2009).
[24] D. J. Reilly *et al.*, Appl. Phys. Lett. **91**, 162101 (2007).
[25] W. Yao, R.-B. Liu, and L. J. Sham, Phys. Rev. B **74**, 195301 (2006); C. Deng and X. Hu, Phys. Rev. B **73**, 241303(R) (2006); L. Cywinski, W. M. Witzel, and S. Das Sarma, Phys. Rev. B **79**, 245314 (2009); Phys. Rev. Lett. **102**, 057601 (2009).
[26] A linear fit of $V_L(B_0)$ is used over the limited range.
[27] D. J. Reilly *et al.*, Phys. Rev. Lett. **101**, 236803 (2008).
[28] C. Deng and X. Hu, Phys. Rev. B **72**, 165333 (2005).
[29] J. A. McNeil and W. Gilbert Clark, Phys. Rev. B **13**, 4705 (1976).
[30] A. Imamoglu *et al.*, Phys. Rev. Lett. **91**, 017402 (2003).
[31] S. I. Erlingsson, Y. V. Nazarov, and V. I. Fal'ko, Phys. Rev. B **64**, 195306 (2001).
[32] I. A. Merkulov, A. L. Efros, and M. Rosen, Phys. Rev. B **65**, 205309 (2002).
[33] W. M. Witzel and S. Das Sarma, Phys. Rev. B **74**, 035322 (2006).
[34] D. Klauser, W. A. Coish, and D. Loss, Phys. Rev. B **78**, 205301 (2008).
[35] J. M. Taylor *et al.*, Phys. Rev. B **76**, 035315 (2007).